ATP Signaling in the Integrative Neural Center of Aplysia Californica

János Györi
Balaton Limnological Institute
Andrea Kohn
University of Florida
Daria Romanova
Russian Academy of Sciences
Leonid Moroz (moroz@whitney.ufl.edu)
University of Florida

Research Article

Keywords: P2X receptors, Bioenergetics, Mollusca, Evolution of Neurotransmitters, Homeostasis, Ion channels, RNA-seq

Posted Date: January 13th, 2021

DOI: https://doi.org/10.21203/rs.3.rs-142396/v1

Version of Record: A version of this preprint was published at Scientific Reports on March 9th, 2021. See the published version at https://doi.org/10.1038/s41598-021-84981-5.

ATP signaling in the integrative neural center of *Aplysia californica*

János Györi[1¶], Andrea B. Kohn[2¶], Daria Y. Romanova[3], Leonid L. Moroz[2,4¶*]

[1]Centre for Ecological Research, Department of Experimental Zoology, Balaton Limnological Institute, H-8237 Tihany, Hungary;
[2]Whitney Laboratory for Marine Bioscience, University of Florida, St. Augustine, FL, 32080,USA;

[3]Institute of Higher Nervous Activity and Neurophysiology, Moscow, 117485, Russia;
[4]Departments of Neuroscience and McKnight Brain Institute, University of Florida, Gainesville, FL, 32610,USA

¶-equal contribution

*****Corresponding author

Emails:moroz@whitney.ufl.edu
https://orcid.org/0000-0002-1333-3176

Running title: ATP modulation in *Aplysia*

Keywords: P2X receptors; Bioenergetics; Mollusca; Evolution of Neurotransmitters; Homeostasis; Ion channels, RNA-seq

#The manuscript is dedicated to Geoffrey Burnstock (1929–2020), who discovered and promote purinergic signaling over decades

Abstract:

ATP and its ionotropic P2X receptors are components of the most ancient signaling systems. However, little is known about the distribution and function of purinergic transmission in invertebrates. Here, we cloned, expressed, and pharmacologically characterized P2X receptors in the sea slug *Aplysia californica* – the prominent neuroscience model. *ac*P2X receptors were successfully expressed in *Xenopus* oocytes and were displayed activation by ATP with two-phased kinetics and Na^+-dependence. Pharmacologically, they were quite different from other P2X receptors. The ATP analog, Bz-ATP, was a less effective agonist than ATP, and PPADS was a more potent inhibitor of the *ac*P2X receptors than the suramin. *ac*P2X were uniquely expressed within the cerebral F-cluster, which contains multiple secretory peptides (e.g., insulins, interleukins, and potential toxins), ecdysone-type receptors, and a district subset of ion channels. We view F-cluster as the multifunctional integrative center, remarkably different from other neurosecretory cells. *ac*P2X receptors were also found in the chemosensory structures and the early cleavage stages. Therefore, in molluscs, rapid ATP-dependent signaling can be implicated both in development and diverse homeostatic functions. Furthermore, this study illuminates novel cellular and systemic features of P2X-type ligand-gated ion channels for deciphering evolution of neurotransmitters.

Graphical Abstract:

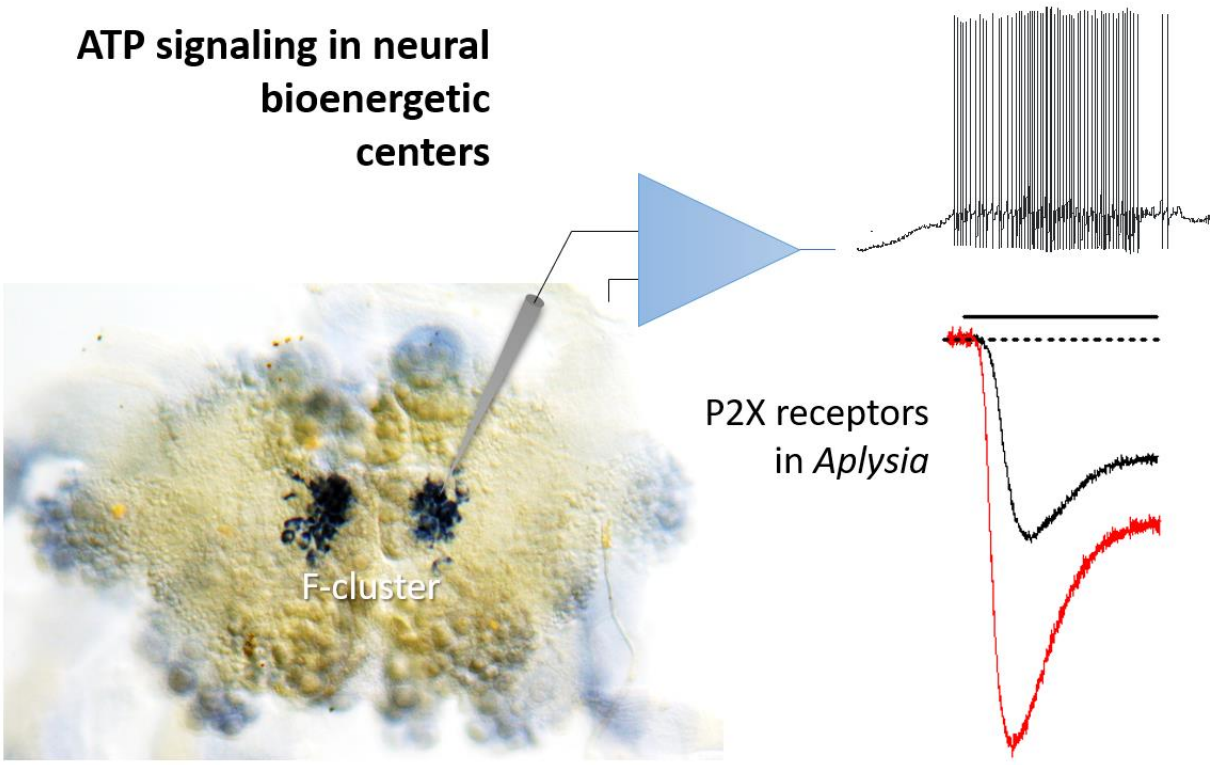

We show that ATP and its ligand-gated P2X receptors are essential signaling components within both the chemosensory systems and the unique integrative neurosecretory center, present in the CNS of the sea slug *Aplysia* – a prominent model in neuroscience. Expression and pharmacology of P2X receptors in *Aplysia* confirms the preservation of evolutionary conserved bioenergetic sensors across animals and provide new tools to decipher homeostatic mechanisms in neuro-endocrine systems in general.

In addition to being the critical energy storage for every cell, ATP acts as one of the most ancient intracellular and intercellular signal molecules[1-3]. The possible involvement of ATP in signaling mechanisms was initiated in the 1920s by Drury and Szent-Gyorgyi[4]; and then in the 1950s by Holtons[5-7], leading to the concept of purinergic transmission in the 1970s by Burnstock[3,8]. Eventually, in 1983, rapid ATP-gated ion currents were discovered in neurons[9,10] and muscles[11], and specific subtypes of the ligand-gated P2X receptors were identified in the 1990s[12-15]. Finally, the 3D structure of P2X receptors was revealed in 2009-2012[16,17]. These are distinctive trimeric ligand-gated channels showing a common architecture with acid-sensing ion channels but unrelated in their respective amino acid sequences[18].

Comparative studies established that P2X-type receptors are broadly distributed across many eukaryotic lineages[1,19-21], including the majority of Metazoa[2,3]. Across all domains of life, ATP can operate as the *bona fide* ancient signal molecule (and a volume transmitter) associated with adaptive reactions to injury and damage[2,3,22].

Nevertheless, the recruitment of P2X receptors into different signaling mechanisms and tissues occurred relatively randomly. In selected evolutionary lineages, P2X receptors were secondarily lost. The list includes higher plants[3], some basal bilaterians such as acoels[22], arthropods and nematodes. For example, *Drosophila* and *C. elegans* genomes have no P2X receptors, but other ecdysozoans such as *Daphnia*, the shrimp *Litopenaeus*, the tick *Boophilus*[23], and tardigrades[24] contain one receptor. Lophotrochosoans or Spiralia, including flatworms, also have one type of P2X receptor with shared pharmacological properties to mammals[25]. However, practically nothing is known about the functional roles of P2X receptors in the CNS and peripheral tissues of invertebrates and molluscs, in particular[3]. Mollusca is one of the most diverse animal phyla in terms of its morphological and biochemical adaptations.

The release of ATP from the central ganglia of the pond snail, *Lymnaea stagnalis,* was demonstrated[26], and, subsequently, P2X receptors were identified in this species with widespread expression across the CNS[27] but unknown function(s).

Here, we show that ATP and its ligand-gated P2X receptors are essential signaling components within chemosensory structures and the unique integrative neurosecretory center present in the CNS of the sea slug *Aplysia* – an important model for neuroscience[28,29]. Expression and pharmacology of P2X receptors in *Aplysia* confirms the preservation of evolutionary conserved bioenergetic reporter-sensor systems across animals and provides new tools to decipher homeostatic mechanisms in neuroendocrine systems and development.

Results

Identity, phylogeny, tissue-specific expression, and quantification of *Aplysia* P2X (AcP2X) receptors

We identified and cloned a single P2X receptor with two splice forms (GenBank#: NP_001191558.1, NP_001191559.1), which shared 92% identity (Supporting Information). The predicted structure of the *Aplysia* P2X receptor reveals all major evolutionary conservative sites and posttranslational modifications (Supporting Information, **Fig. 1S**), which are similar to its homolog in another gastropod, *Lymnaea*[27]. The genomic organization of the P2X receptors confirmed the overall evolutionary conservation of exons and intron-exon boundaries. *Aplysia* P2X receptor exons are similar in number and length to other vertebrate P2X4 receptors, but it is not correct in some other invertebrates (Supporting Information, **Fig. 2S**).

Fig. 1*A* shows the phylogenetic relationships among P2X receptors with distinct events of gene duplications in the lineages leading to humans, zebrafishes, hemichordates, echinoderms, and basally-branched metazoans such as sponges, placozoans, and cnidarians. In contrast, representatives of molluscs (including *Aplysia*), annelids, and parasitic flatworms (*Schistosoma*) appear to have a single copy of a P2X-encoded gene that often form distinct phyletic clusters within a respective phylum. This reconstruction suggests a single P2X gene in the common metazoan ancestor with independent multiplication events in selected animal lineages. It primarily occurred within vertebrates as the reflection of whole-genome duplications early in the evolution of this group. Interestingly, some bilaterians such as the acoel *Hofstenia miamia*, insects, and nematodes[30] secondarily lost the P2X receptors. This mosaic-type phyletic distribution likely illustrates different system constraints for recruiting P2X receptors to novel functions or preserving ancestral molecular mechanisms of purinergic signaling.

Next, we characterized the expression of the P2X receptors in *Aplysia* using a broad spectrum of RNA-seq data obtained from adult and developmental stages[31] (see Supporting Information, Table 1S). The highest level of *AcP2X* expression was found in the chemosensory structures (the mouth area and rhinophores[32] as well as in the gill (**Fig. 1*B***), which is also known as the chemosensory and respiratory organ. Expression of *AcP2X* receptors was also detected in the majority of peripheral organs of *Aplysia* as well as during the first cleavage stages (**Fig. 1*B***), where no neurons or specialized sensory cells exist. Thus, ATP could act as a paracrine messenger in early embryogenesis.

The freshwater pond snail *Lymnaea stagnalis* is the only know molluscan species with the biophysical characterization of P2X receptors[27]. The structural organization of the *Aplysia* P2X receptor was comparable to *Lymnaea*'s P2X (**Fig. 1C, Fig. 2**; and **Fig. 3S** Supplementary Information) but with noticeable differences in their predicted ATP binding and other regulatory sites suggesting potentially different biophysical and pharmacological properties. These differences are also evident in the 3D models for related molluscan species (**Fig. 2** and **Fig 3S**, Supplementary Information), which suggest that marine and freshwater organisms are different in the kinetic and pharmacological properties of their respective P2X receptors. This possibility was experimentally tested, as we reported below.

Expression of AcP2X in *Xenopus* oocyte confirms the evolutionary conservation of kinetic and pharmacological parameters

ATP elicited an inward current in a concentration-dependent manner in oocytes injected with *AcP2X* (**Fig. 3*A***). EC_{50}s were determined for both the fast- (0-1seconds) and the slow component of current with continuous application of ATP. The EC_{50} for the fast component was 306.0 µM with a 1.58 Hill coefficient, and for the slow component, 497.4 µM with a 0.97 Hill coefficient (n=5 oocytes, **Fig. 3*B***). The second application of the agonist, with a recovery time of 6 minutes, generated a 15-30% reduction in peak amplitude and is indicative of the rundown observed in other P2X receptor subunits. The response to 250 µM ATP produced a mean peak amplitude of 31.3 nA$\pm$3.8 nA and a time to a peak value of 2.76±0.21s (n=19) with a holding membrane potential of -70 mV (**Fig. 2*C***). The ATP analog, 2',3'-O-(4-Benzoylbenzoyl) adenosine 5'-triphosphate (Bz-ATP[33]) gave a partial response at 20% of the ATP response (n=8 oocytes, **Fig. 3*C***). There were no UTP and ADP responses within the same range of concentrations (data not shown).

The current-voltage relationship was investigated in the presence of elevated (144 mM) and low extracellular NaCl (96 mM) concentrations (n=6 oocytes, **Fig. 3*D***). A reversal potential was determined by applying a ramp protocol from -70mV to 20mV in high and normal Na^+ with 250μM of ATP (**Fig. 3*E***). According to the Nernst equation, the reversal potential was 13.9mV and shifted by +10.2+1.3mV to positive holding in high sodium solution (n=6 oocytes).

P2X antagonist suramin[33] inhibited ATP responses in a concentration-dependent manner (**Fig. 4 *A,B***; 7 oocytes). Another P2X antagonist, pyridoxal-phosphate-6-azophenyl-2',4-disulfonic acid (PPADS[33]), also inhibited the response of ATP on *Ac*P2X in a concentration-dependent manner (**Fig. 4*C,D***). However, the application of PPADS produced a greater block than the suramin (**Fig. 4*E***). Mean current responses to 250 μM ATP in the range of 1-250 μM PPADS generated an EC_{50}=211.2 μM for the fast component, but the slow component could not be calculated (5-7 oocytes, **Fig. 4*D***). The second splice form of *Ac*$P2X_b$was also expressed in oocytes producing currents very similar to the first isoform *Ac*P2X described above; however, it resulted in much smaller (and unstable) responses (data not shown).

P2X receptors are expressed in unique populations of neurosecretory cells of *Aplysia*

Interestingly, the CNS has the overall lowest *P2X* gene expression (**Fig. 1*B***). This situation might be analogous to the recruitment of purinergic signaling in the chemosensation within the mammalian brain[34], suggesting a distinct and relatively small population of ATP-sensing cells. We tested this hypothesis.

AcP2X was explicitly expressed in two symmetrical subpopulations of insulin-containing neurons (**Fig. 5*A***, n=6) localized in the F-cluster in the cerebral ganglion of *Aplysia*[35,36]. Each subpopulation contained about 25-30 electrically coupled cells (30-50 μm diameter, **Fig. 5*A-B***)[35]. Application of 2 mM ATP to these neurons elicited a 2-5 mV depolarization, action potentials, and these effects were reversible (**Fig. 5*C***) and voltage-dependent (**Fig. 5*D***), consistent with the pharmacological properties of *Aplysia*'s P2X receptors expressed in oocytes. Neurons that were negative for *AcP2X* by *in situ* hybridization showed no response to as high as 10 mM ATP concentration.

These tests confirmed that P2X receptors in F-cluster neurosecretory cells are functional. Next, using the RNA-seq approach, we investigated this cluster's molecular organization and compared it with other neurosecretory cells to get insights into potential functions of this unique cell population.

Unique molecular organization of P2X-expressing neurosecretory cells

Using RNA-seq, we compared the F-cluster transcriptome (**Fig. 6*A***) to other neurosecretory cells with a similar overall morphological organization, such as the bag cluster neurons (**Fig. 6*B***) in the abdominal ganglion[37]. Neurons from both of these clusters are the most prominent secretory cells in the entire organism (**Fig. 6*D***); both groups of cells release their secretes in neurohaemal areas along the nerves, and their connective tissues[35,37] but their molecular (and perhaps systemic) functions are remarkably different. This situation is clearly reflected in their distinct transcriptome profiles (**Fig. 6**, and Supplementary Information **Figs 4S-7S**).

The neurosecretory bag cells induce and integrate complex egg-laying behaviors due to the release of several secretory peptides[38-40]. Predictably, all of them were highly expressed in our RNA-seq dataset (**Fig. 6*B***, Supporting information, Table 2S), there were 7213 genes expressed only in bag cluster, including a distinct (from F-cluster) isoform of *insulin*, *aerolysin* 1-toxin-like peptide, and a diverse set of ion channels (**Fig. 6*C*** and ***E*,** Supplementary Information, Table 2S).

In contrast to bag cells, very little is known about P2X expressing F-cluster neurons. It was shown that these cerebral neurons contain insulin and have broad secretory areas with a likely non-synaptic hormone release in the connective tissues, nerves, and circulatory system[36]. It was suggested that these neurons might be involved in glucose control[41] and perhaps reproduction, with likely hormonal interactions to the bag cells.

There are 5159 genes differentially expressed in F-cluster (Supplementary Information, Table 2S). Our RNA-seq data (**Fig. 6*A***, Supplementary Information, Table 2S) also revealed that F-cluster neurons expressed three distinct *insulins*, *cerberin*, and at least 4 novel secretory neuropeptides as well as toxin-like peptides. The most surprising finding in F-cluster neurons was an extremely high level of expression of *interleukin 17A*-like (a pro-inflammatory cytokine[42]) and *interferon α-inducible protein 27* (*IFI27*), originally known to be involved in innate immunity, and is later found to intervene in cell proliferation. An *Aplysia*-type ecdysone receptor was also differentially expressed in F-cluster neurons (compare to bag-cells) consistent with expression of many components of steroid hormone machinery in *Aplysia* (Supplementary Information, Table 2S). In contrast to bag cells, we found evidence of innervation of F-cluster neurons by about a dozen neuropeptides (*FMRFa*, *FIRFa*, *Pleurin*, *MIP*, *AGN5*, *CCN-amide, PRQFVa*, *L11*, *CP2*, *Allatotropins*, *APGWA*) including *sensorin* from nociceptive neurons [43]. In each of these cases, it is known[36,41,44,45] that these neuropeptide prohormones are expressed in different neuronal populations (our *in situ* hybridization for these transcripts, not shown), but respective precursor mRNAs are transported to distant neurites[45], and these extrasomatic RNAs are detected from synaptic regions on target neurons.

Of note, two neuropeptide inputs can be mediated by *seductin* (a pheromone involved in the integration of reproductive behaviors[46-48] and *enterin* (myoactive factors[49-52]) are apparently shared between F-cluster and bag cells (**Fig. 6*A*, *B***). The presence of insulin receptors in bag cells implies long-distance interactions between F-cluster neurons and bag cells.

Non-coding RNAs also showed differential expression between clusters (Supplementary Information, Table 2S).

Discussion

As the central bioenergetic currency, the intracellular concentrations of ATP reach 1-10 mM with multiple mechanisms of its extracellular release across all domains of life[2]. In the molluscan CNS, the baseline level of ATP release can be increased following depolarization and serotonin application, suggesting that ATP can act as an endogenous fast neurotransmitter[26]. The presence of ionotropic P2X ATP-gated cationic channels in peripheral chemosensory structures (together with profound serotonergic innervations of these structures[53]) and the CNS (**Fig. 1*B***) further support this hypothesis. However, we also reported *AcP2X* receptor expressions early in development, suggesting that ATP might be a paracrine signal molecule controlling cleavage and differentiation.

The purinergic sensory transmission is widespread in mammals[34] and might have deep evolutionary roots[2,3,22]. Mammalian P2X receptors[13] are comparable to their homologs in *Aplysia* based on their sequence and kinetic parameters but have a lower sensitivity to ATP. As a part of

future directions in comparative biophysical studies, it would be important to perform targeted mutagenesis of the molluscan P2X receptors to precisely identify amino acids responsible for the observed differences among mammalian and invertebrate P2X receptors.

The overall kinetic and pharmacological parameters of *Aplysia* P2X receptors are also similar to those described both in the closely related *Lymnaea*[27] and distantly related *Schistosoma*[25]. However, the *Lymnaea* P2X receptor showed much higher sensitivity (EC_{50} is in μmolar range) to ATP than *Aplysia*, consistent with predicted structural differences of P2X receptors across species (**Figs. 1-2**). Suramin and PPADS both inhibited the ATP evoked responses in other species[23-25,27], but in *Aplysia,* it occurred in a narrower range (10-250 μM) than in *Lymnaea* (0.1 μM-250 μM). Suramin and PPADS are known as pan-P2X blockers. Thus, it might be expected that novel and, perhaps, more selective antagonists could exist for the *Aplysia* receptor subtype.

Ecdysozoan P2X receptors are also relatively diverse (although detailed mutagenesis studies have not been performed in any representatives of this largest metazoan lineage). In contrast to *Aplysia*, the tick P2X receptor displayed a very slow current kinetics and little desensitization during ATP application[23]. The tardigrade P2X receptor[24] had a relatively low sensitivity for ATP (EC_{50} ~44.5 μM), but fast activation and desensitization kinetics – similar to *Aplysia*.

In summary, *Aplysia* P2X receptors exhibit a distinct phenotype, having a moderate ATP sensitivity (compared to the freshwater *Lymnaea* and mammals) but faster kinetics than some ecdysozoans. These "hybrid features" might be related to the marine ecology of *Aplysia* with a wider range of environmental changes. The agonist potencies (ATP and BzATP) in the cloned *Aplysia* P2X do not match any known P2X receptor subtype. It suggests that there was a specific diversification of P2X receptors in the lineage leading to *Aplysia*.

Also, the currents recorded from the *Aplysia* F-cluster neurons do not fully resemble the currents recorded from the oocytes. They do not desensitize, and they get bigger as the membrane potential hyperpolarizes. These observations also suggest that either expression in *Xenopus* (as the freshwater animal with different osmolarity) modify the properties of native channels or implicated additional regulatory mechanisms for the *Aplysia* P2X receptors in the intact CNS. Additional integrative analyses would be needed to biophysically determine the channel properties and physiological role of AcP2X receptors.

Interestingly, the abundance of P2X receptors in the *Aplysia* chemosensory systems (such as mouth areas, rhinophores, and gills) correlates with the expression of nitric oxide synthase[54], suggesting interactions of these afferent pathways in the control of feeding and respiration. *Aplysia* might also detect environmental ATP from bacterial and algal (food) sources[2] as in some other studied marine species, including lobsters[55].

Within the CNS of *Aplysia*, P2X receptors are expressed in the distinct cluster of insulin-containing neurons[35,36], likely associated with the systemic control of growth and, subsequently, reproduction. The potential functional roles of many differentially expressed genes in F-cluster could be determined in the future, but their involvements in control of multiple behaviors, immunity is evidenced by a broad array of respective genes uniquely or differentially expressed in F-cluster (Supplementary Information, Table 2S). This is the reason to view this cluster as one of the top-level integrative centers in the animal with the broadest spectrum of secretory peptides and multiple receptors, including P2X receptors.

The release of the *Aplysia* insulin can decrease the level of glucose in the hemolymph[36]. Moreover, F-cluster neurosecretory cells are electrically coupled[35], which help synchronize their discharges and, eventually, insulin secretion. It is known that ATP can also be released from gap

junctions (innexins) and during synaptic exocytosis[2]. Thus, we can propose that P2X-induced neuronal depolarization of insulin-containing neurons provide positive purinergic feedback sustaining the excitability and secretory activity of this multifunctional integrative center in *Aplysia* and related gastropods.

Second, the currents recorded from the *Aplysia* F-cluster neurons do not fully resemble the currents recorded from the oocytes. They do not desensitize, and they get bigger as the membrane potential hyperpolarizes.

In summary, the observed diversity of specific transcripts controlling pain, injury, toxins, immunity feeding, reproduction, and energetics, together with ATP-sensitivity suggests that F-cluster can represent a neurosecretory integrative center, controlling (at least in part by purinergic signaling) a broad majority of the animal's behavior and functions.

Materials and Methods

Animals and molecular analyses of *Aplysia* AcP2X

Aplysia californica (60-100 g) were obtained from the National Resource for *Aplysia* at the University of Miami (Supplementary Information for details). The original sequences were generated using RNA-seq profiling[41,44,45,56]. Details for RNA extraction and cDNA library construction have been described[41,44,56,57] and provided in Supplementary Information. We used the same protocols for whole-mount *in situ* hybridization as reported elsewhere[58,59] with a specific probe for the validated *Ac*P2X (Supplementary Information). Expression of *AcP2X* was performed in eight experimental and two control preparations of the CNS; additional controls were reported elsewhere[44,59]. Control *in situ* hybridization experiments with full length 'sense' probes revealed no specific or selective staining under identical labeling protocols. Images were acquired with a Nikon Coolpix4500 digital camera mounted on an upright Nikon Optiphot-2 microscope.

Expression levels of transcripts were calculated using the normalization method for RNA-seq - Transcripts Per Million (TPM)[60]. Mapping was performed in the STAR (2.3.0)/feature Counts analysis with the values obtained from the Bowtie2/Tophat pipeline[61]. The mapped reads were summarized and counted within the R statistical programming language. Supplementary Information, Table 1S contains a list RNA-seq projects and their corresponding SRA number.

Electrophysiology

Oocytes recordings. RNA preparation for oocyte injections and oocyte maintenance are found in Supplementary Information. The oocyte recording bath was in ND96 medium (96 mM NaCl, 2 mM KCl, 1 mM $MgCl_2$, 1.8 mM $CaCl_2$, and 5 mM HEPES, pH=7.4), or with the 1.8mM $CaCl_2$ being replaced by 1.8 mM $BaCl_2$. Ba^{2+} was used in oocytes experiments only to block the endogenous chloride and potassium currents in *Xenopus* oocytes. Whole-oocyte currents were recorded by two-electrode voltage clamp (GeneClamp500B, Axon Instruments, Foster City, CA, USA) using microelectrodes made of borosilicate glass (WPI, USA) with a resistance of 0.5–1 MΩ when filled with 2.5 M KCl. Currents were filtered at 2 kHz and digitally sampled at 5 kHz with a Digidata 1320B Interface (Axon Instruments, CA). Recording and data analysis were performed using pCLAMP software version 8.2 (Axon Instruments). For data acquisition and clamp protocols, the amplifiers were connected via a Digidata 1320B AD/DA converter (Axon,

USA) to an AMD PC with pClamp 8.2 voltage-clamp software (Axon, USA). Unfiltered signals were sampled at 10 kHz and stored digitally.

Data are presented as mean±S.E. using Student's paired *t*-test. Concentration-response data were fitted to the equation $I=I_{max}/[1+(EC_{50}/L)^{nH}]$, where I is the actual current for a ligand concentration (L), n_H is the Hill coefficient, I_{max} is the maximal current and EC_{50} is the concentration of agonist evoking 50% the maximum response. To compute the reversal potential for sodium, the Nernst equation used; Vj=(RT)/(zF)ln(c1/c2) where R is the gas constant 1.98 $calK^{-1}mol^{-1}$, F is the Faraday constant 96,840 C/mol, T is the temperature in ^oK and z is the valence of the ion.

***In situ* recordings**. Voltage- and current-clamp experiments were carried out on identified F-cluster neurons in intact nervous systems of *Aplysia*[35]. ~0.5 mL bath was perfused with solutions (artificial sea water) using a gravity-feed system and a peristaltic pump, and solution exchanges were performed by VC-6 six-channel valve controller (Warner Inst., USA). Conventional two-electrode (3-10 MΩ) voltage-clamp techniques (Axoclamp2B, TEVC mode) were employed to measure agonist-activated currents as reported[62] at room temperature(20±2^{o}C). To characterize membrane and action potentials, we used a bridge mode of Axoclamp2B with borosilicate microelectrodes (tip resistance:10-18 MΩ, with 0.5 M KCl, 2 M K-Acetate, and 5 mM HEPES, pH=7.2).

RNA-seq. The isolation of specific cells, RNA extraction and preparation of cDNA for RNA-seq analysis as well as transcriptome annotation has been performed using the same methods as reported elsewhere[41,44,56,57].

Protein modeling. The reconstruction of 3D-structures of the P2X receptor from *Aplysia californica* (NP_001191558.1, GenBank, NCBI) and *Lymnaea stagnalis* (AFV69113.1, Genbank, NCBI) was based on pdb ID: 5svk (open state) and 4dwo (closed state) modeling[63]. Alternative models of the same P2X receptors were generated using PyMol (The PyMol Molecular Graphics System, Version 1.8.6.0 Schrödinger, LLC) and Phyre2 software[63-66].

Data availability

All data are contained within the article as well in Supplementary Information.

Acknowledgments

We thank Dr. T.Ha and E. Bobkova for help with cloning and *in situ* hybridization.

Author contributions

All authors had access to the data in the study and take responsibility for the integrity of the data and the accuracy of the data analysis. Research design, acquisition of data: all authors. Molecular data, expression and RNA-seq: A.B.K., L.L.M.; Protein modeling and analysis: D.R. Pharmacological tests: J.G.; Analysis and interpretation: all authors: Manuscript writing: L.L.M. Funding: L.L.M.

Funding and additional information

This work was supported by the Human Frontiers Science Program (RGP0060/2017) and National Science Foundation (1146575,1557923,1548121,1645219) grants to L.L.M. Research reported in this publication was supported by the National Institute of Neurological Disorders and Stroke of the National Institutes of Health under Award Number R01NS114491 (to L.L.M.). The content is solely the responsibility of the authors and does not necessarily represent the official views of the National Institutes of Health.

Conflicts of interest

The authors declare no conflict of interest.

Figures and Legends

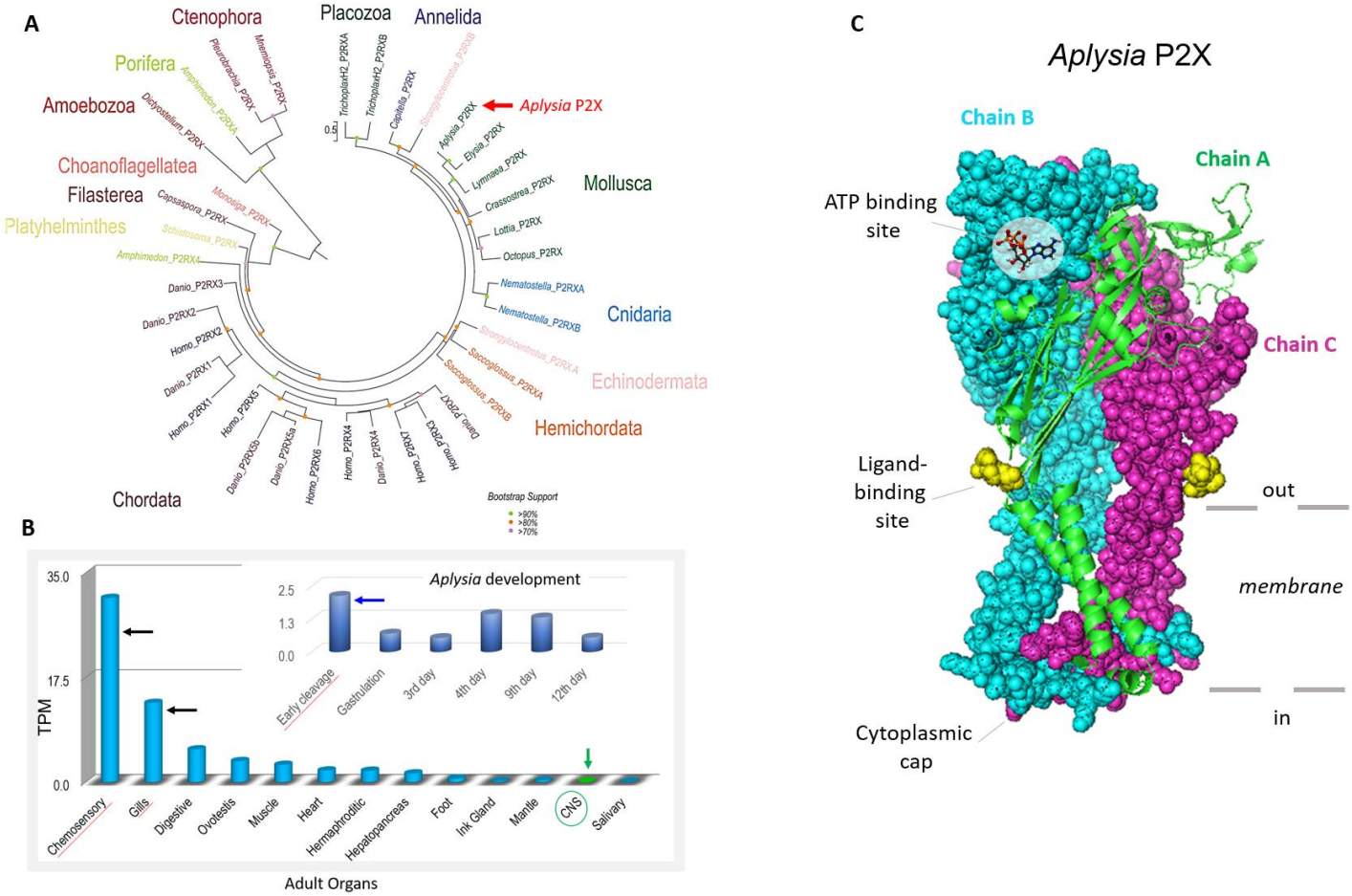

Figure 1. A. **Phylogenetic relationships of P2X and P2X-like receptors (P2RX). *A*.** A maximum likelihood (ML) phylogenetic tree of P2X receptors (Supplementary Information for sequences and accession numbers) with the best-fit model (LG+G). Bootstrap support less than 70 omitted. Phylogenetically, the P2X predicted proteins cluster by phyla. P2X-type receptors are not unique to metazoans because they are detected in unicellular green algae *Ostreococcus tauri* [20], the amoeba *Dictyostelium discoideum* [19] the unicellular eukaryote *Monosiga brevicollis* [20], as well as Capsaspora owczarzaki (21), and all these species, appear to have one P2X gene. Most of the non-bilaterians seem to have at least two P2X receptors (except for ctenophores, where only one receptor was detected). Lophotrochozoans, including the mollusc *Aplysia* and kins, appear to have one P2X receptor with different isoforms. The sea urchin and the acorn worm, *Saccoglossus,* both have at least two genes but numerous isoforms [1]. Humans [13], as well as other chordates, appear to have seven unique P2X receptor genes [1]. ***B.*** Quantification of the expression of P2X receptors in the CNS, peripheral tissues, and developmental stages (insert) of *Aplysia*. The RNA-seq data represented as TPM (transcript per million) values [67-69]. The highest expression levels were detected in chemosensory areas (mouth areas and rhinophores), gills, and early developmental

stages (Supplementary Information, Table 1S for RNA-seq projects). ***C***. 3D modeling for P2X

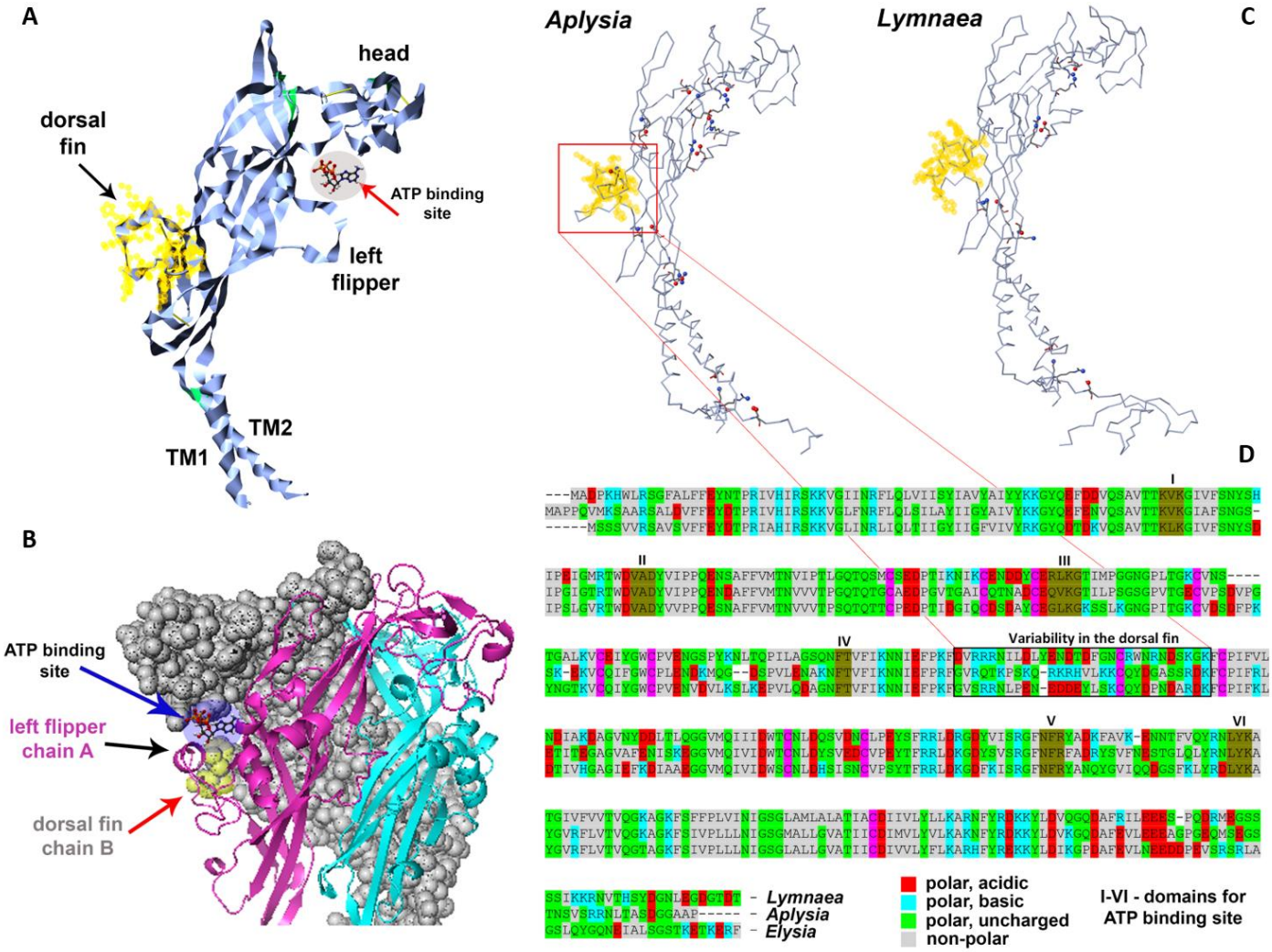

receptor of *A. californica* (model PDB: 5svk).

Fig. 2. The organization of the P2X receptor in *Aplysia californica*. *A* and *B*. Structural features of the P2X monomer models with regions recognized for mammalian homologs in crystallography studies [16,17]. TM1 and TM2 are transmembrane regions (see **Fig. 1C**). ***B***. 3D modeling of the trimeric P2X organization with suggested functional regions[16-18,70]. 'Left flipper' (chain A) and 'dorsal fin' (chain B) together with a head (chain A) of these chains form the ATP binding site (see also **Fig. 1*C***). ***C***. Comparisons between *Aplysia* and *Lymnaea* receptors (open state) based on the difference of salt bridges (yellow – 'dorsal fin'). ***D***. The alignment for P2X receptors in gastropod molluscs (*Aplysia californica*, *Lymnaea stagnalis* and *Elysia chlorotica*) with domain for the ATP binding site (brown – I-VI domains). Of note, *Aplysia* (middle in the alignment) has significantly less polar acidic and more polar basic amino acids in the 'dorsal fin' region [11pb:2pa] compared to other species (*Lymnaea* [7pb:6pa] and *Elysia* [5pb:8pa]), suggesting different kinetic and pharmacological properties of P2X receptors. In summary, there are 13 polar charged amino acids in the `dorsal fin`.

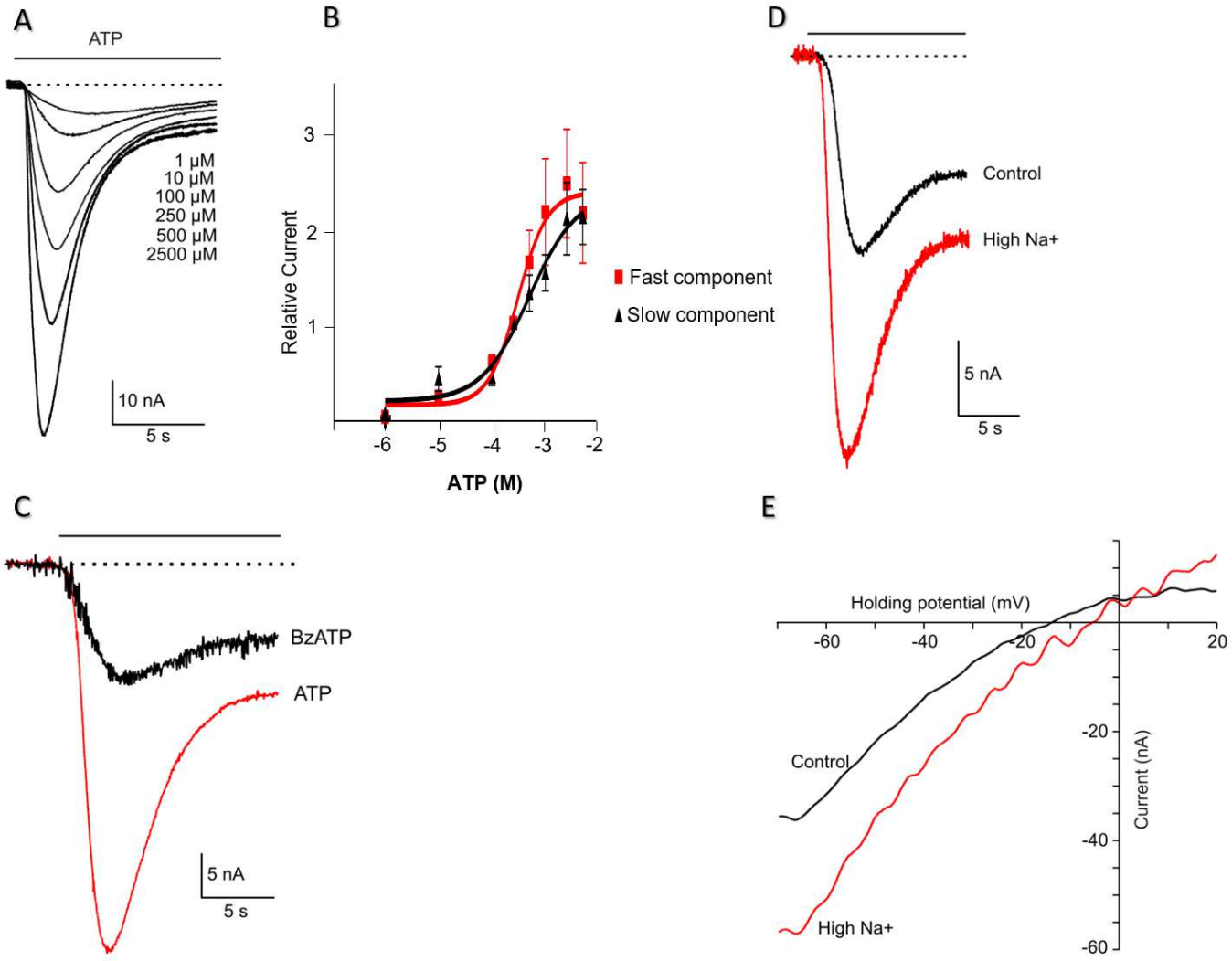

Figure 3. Functional expression of recombinant *Ac*P2X receptors in *Xenopus* oocytes. ***A***. Examples of currents recorded in response to different concentrations of ATP (HP=-70 mV, agonist application indicated by the solid line*)*. ***B***. Dose-response curves for ATP receptor activation. Mean currents were normalized to the response given by 250 µM ATP (*n*=7 oocytes). Serially increasing concentrations of ATP were applied to oocytes for 15 s at 6-min intervals. Symbols represent mean±S.E. Continuous line for *ATP* represents data fitted using the equation I= I_{max}/[1+(EC50/L)*nH*], where I is the actual current for a ligand concentration (L), *nH* is the Hill coefficient, and I_{max} is the maximal current (EC_{50fast} = 306.0 µM, EC_{50slow}= 497.4 µM; nH_{fast}*=1.58,* nH_{slow}*=0.97*). ***C***. Two-electrode voltage-clamp recordings from oocytes expressing *Ac*P2X receptors. Representative inward currents recorded in response to ATP (red trace) and the 250 µM of Bz-ATP (HP=-70 mV, application indicated by the solid line). ***D***. Recordings of ATP-induced current (250 µM, ATP) in the presence of normal [Na^+] (96mM) and with elevated extracellular Na^+ (144 mM; red trace); HP=-70 mV. ***E***. Ramp voltage-clamp protocol from -70 mV HP to 20mV in the presence of 250µM ATP. The plots of the subtracted current (a current in the presence of ATP minus the current in the absence of ATP) against voltage during the ramp. The red trace - high [Na^+], 144 mM. According to the Nernst equation, the reversal potential was shifted by 10.2±1.3 mV to the + direction of the *holding* potential.

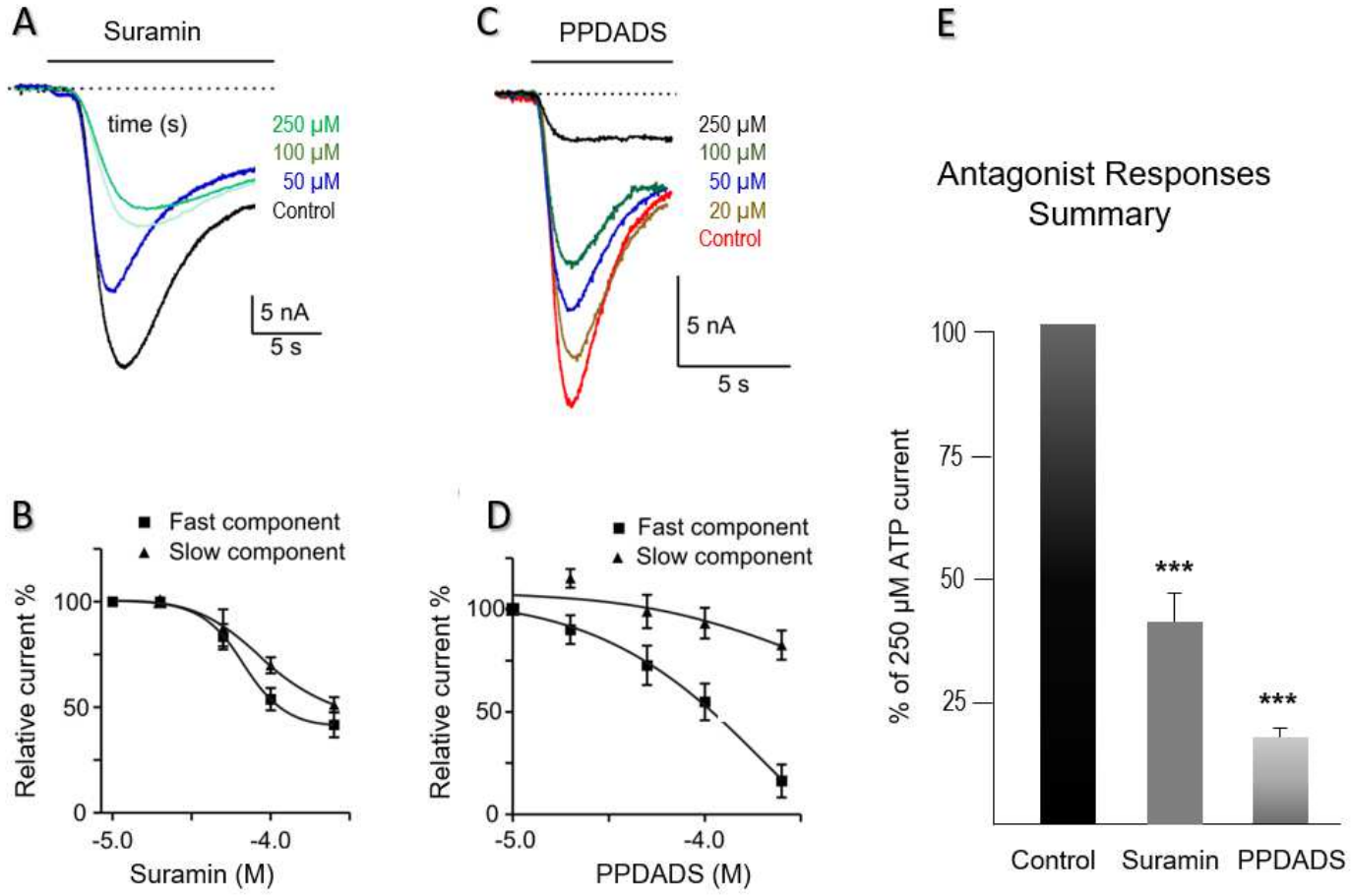

Figure 4. Pharmacology of *Ac*P2X receptors in *Xenopus* oocytes. ***A.*** Example of currents induced by 250 µM ATP. ATP was applied to oocytes for 15 s, in the presence of varying concentrations of suramin (HP=-70 mV). ***B***. Mean responses to 250 µM ATP in the presence of 1-250 µM suramin. There was a suramin-resistant component of the *Ac*P2X current. Symbols represent mean±S.E. ***C***. Traces recorded in response to 250µM ATP in the presence of varying concentrations of the second antagonist, PPADS (concentrations are shown in µM, and all applications are indicated by the solid lines). ***D***. Mean responses to 250µM of ATP in the presence of the PPADS (a fast component of responses - closed squares, slow component - triangles). PPADS was an effective antagonist in the range of 1–250µM. Fitting of the data using the sigmoidal dose-response curve by a continuous line, EC_{50fast}=211.2. Symbols represent the mean±S.E. ***E***. The suramin proved to be a more effective blocker of the ATP-activated channels among the two antagonists tested. A chart of mean currents (% of 250 µM ATP response) in the presence of 250 µM Suramin and 250 µM PPADS. Mean currents were normalized to the response given by 250 µM of ATP. Symbols represent mean±S.E; statistically significant differences (Student's *t*-test) from control (P<0.05) are indicated by asterisks (***) above the bars.

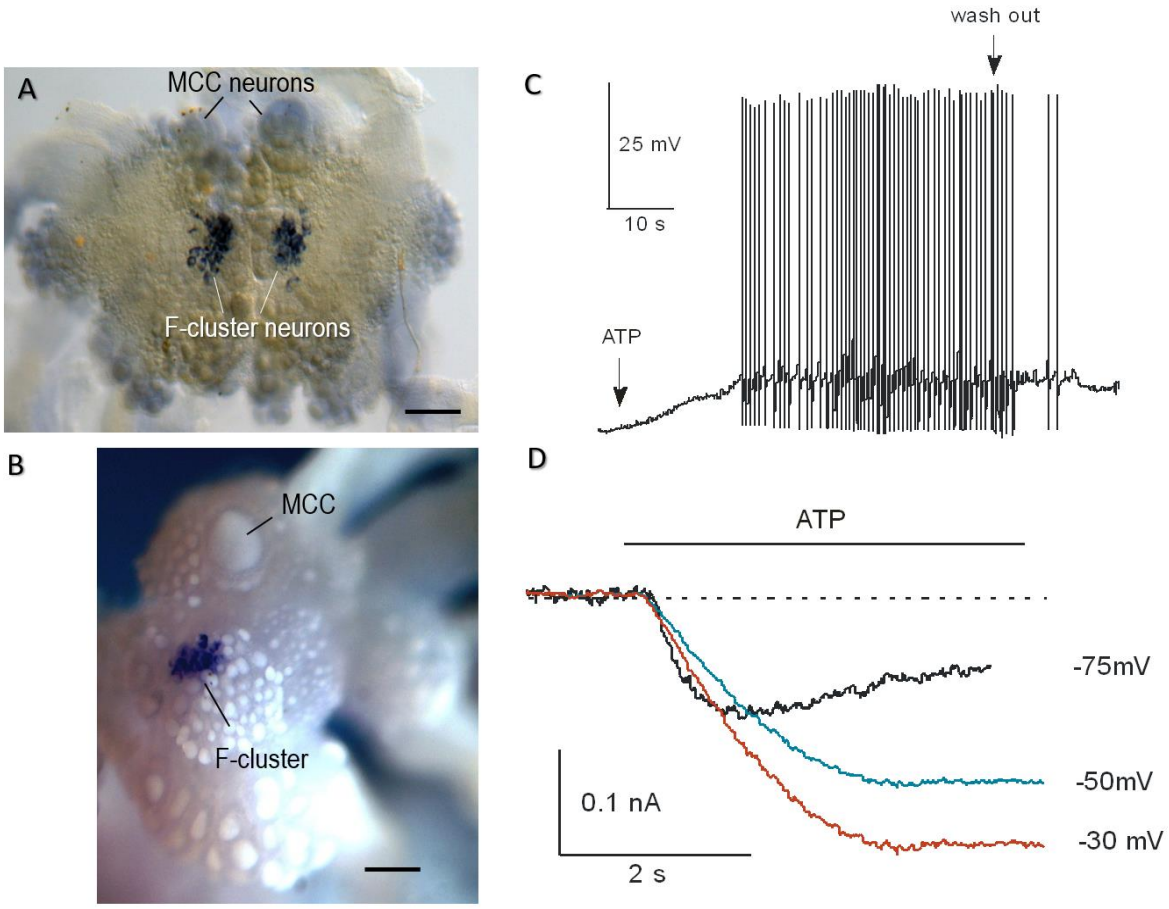

Figure 5. Distribution of *AcP2X* in the CNS of *Aplysia* and the effect of ATP on *Aplysia* F-cluster neurons. ***A*** and ***B***: *AcP2X* is expressed in neurons of the cerebral F-cluster (*in situ* hybridization). A pair of giant serotonergic feeding interneurons (MCC) are indicated by arrows. ***A***. The preparation embedded in a mounting media. ***B***. The cerebral ganglion was photographed in 100% ethanol. Scale: 300 µm. ***C***. Current-clamp recording from F-cluster neurons in the intact CNS. Bath application of ATP (2.0 mM) caused an excitatory response with spiking activity (2-5 mV depolarization with a burst of the action potentials), and full recovery following washout (indicated by arrows). ***D***. Voltage-clamp recording from F-cluster neuron. Raw traces recorded in response to 2.0 mM of ATP at three holding potentials (agonist application indicated by the line).

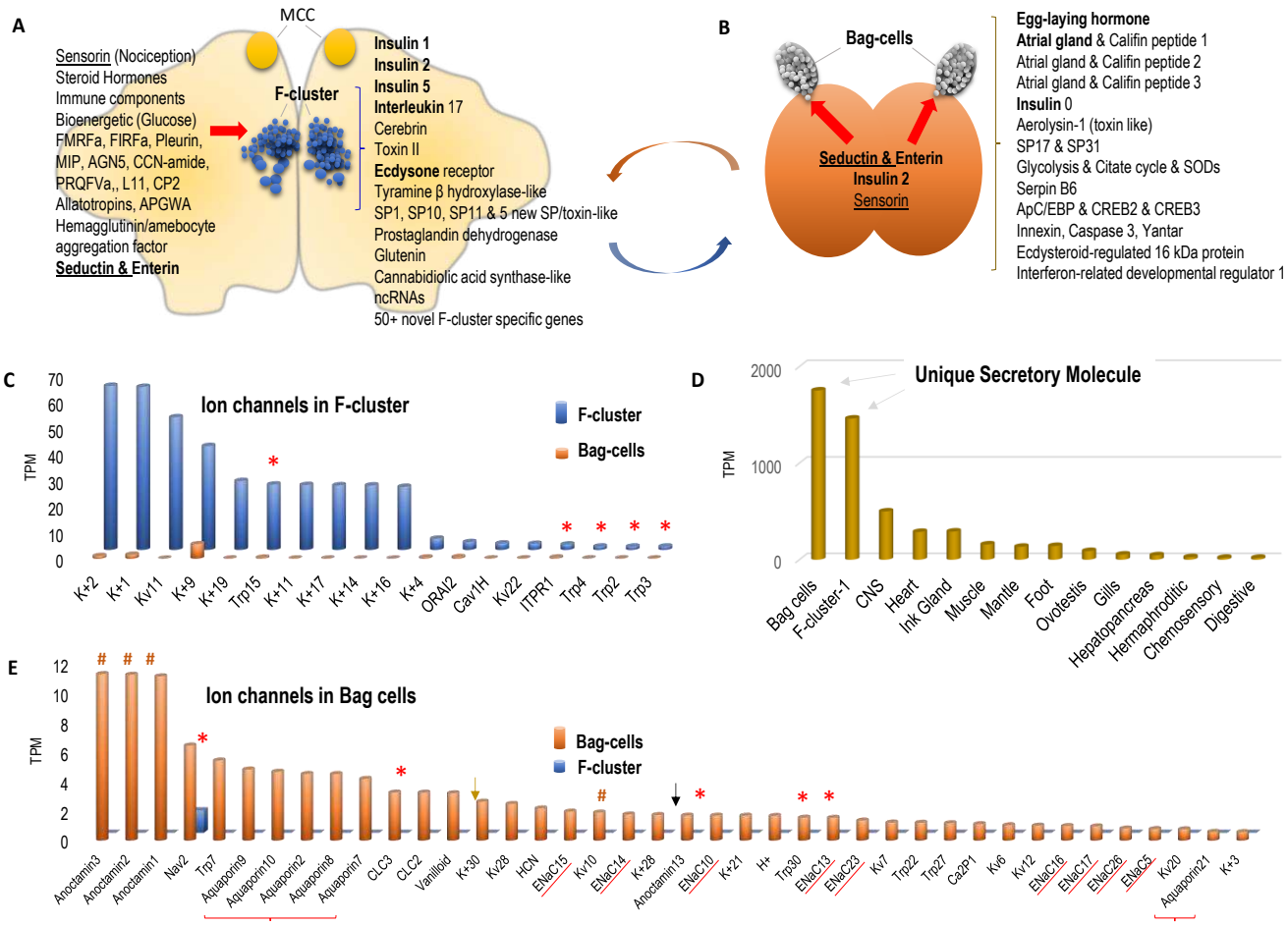

Figure 6. F-cluster and Bag cells are the two most prominent neurohaemal centers in *Aplysia*. ***A.*** Schematic representation of F-cluster in the cerebral ganglion (MCC- serotonergic metacerebral cells involved in feeding arousal) together with genes [on the right, e.g., insulins 1 and 2, interleukin 17, etc.] differentially expressed in this cluster (RNA-seq). Red arrow indicates predicted other peptidergic inputs [on the left] to F-cluster (see text for details). F-cluster is one of the most molecularly heterogenous neurorosecretory clusters in the CNS. ***B.*** Bag cells in the abdominal ganglion with cluster-specific peptides [on the right] expressed in these neurosecretory cells (RNA-seq). Red arrow indicates other peptidergic inputs to bag cells (see text for details). Of note, seductin, enterin, and sensorin inputs are shared (underlined) between these two neurohaemal centers, whereas insulin 2 is produced in the F-cluster. ***C.*** Both bag cells and F-cluster have the highest overall expression of an uncharacterized secretory molecule (XP_005092953.2) compared to other organs. ***D*** and ***E***. Putative ion channels differentially expressed in the F-cluster and bag cells, respectively (see Supplementary Information excel table:Ion channels for F-cluster and Bag cells). Asterisks indicate cluster-specific transient receptor potential (TRP) channels; # - anoctamins,– aquaporins; brown and black arrows HCN and voltage-gated proton channels, respectively. ENaC – are ligand-gated peptide channels (underlined). Other abbreviations: K+ Calcium-activated, Inwardly rectifying, Tandem pore domain potassium channels; Kv voltage-gated potassium chnnels; Nav- voltage-gated sodium channel, Ca2P two pore calcium channels. The numbers in names Do Not infer type of channel but for identification only.

References

1 Hou, Z. & Cao, J. Comparative study of the P2X gene family in animals and plants. *Purinergic Signal* **12**, 269-281, doi:10.1007/s11302-016-9501-z (2016).

2 Verkhratsky, A. & Burnstock, G. Biology of purinergic signalling: its ancient evolutionary roots, its omnipresence and its multiple functional significance. *Bioessays* **36**, 697-705, doi:10.1002/bies.201400024 (2014).

3 Verkhratsky, A. Early evolutionary history (from bacteria to hemichordata) of the omnipresent purinergic signalling: A tribute to Geoff Burnstock inquisitive mind. *Biochem Pharmacol*, 114261, doi:10.1016/j.bcp.2020.114261 (2020).

4 Drury, A. N. & Szent-Gyorgyi, A. The physiological activity of adenine compounds with especial reference to their action upon the mammalian heart. *The Journal of physiology* **68**, 213-237 (1929).

5 Holton, P. The liberation of adenosine triphosphate on antidromic stimulation of sensory nerves. *The Journal of physiology* **145**, 494-504 (1959).

6 Holton, F. A. & Holton, P. The capillary dilator substances in dry powders of spinal roots; a possible role of adenosine triphosphate in chemical transmission from nerve endings. *J. Physiology* **126**, 124-140 (1954).

7 Holton, F. A. & Holton, P. The vasodilator activity of spinal roots. *J Physiol* **118**, 310-327, doi:10.1113/jphysiol.1952.sp004796 (1952).

8 Burnstock, G. Purinergic nerves. *Pharmacol Rev* **24**, 509-581 (1972).

9 Krishtal, O. A., Marchenko, S. M. & Pidoplichko, V. I. Receptor for ATP in the membrane of mammalian sensory neurones. *Neuroscience Letters* **35**, 41-45, doi:10.1016/0304-3940(83)90524-4 (1983).

10 Jahr, C. E. & Jessell, T. M. ATP excites a subpopulation of rat dorsal horn neurones. *Nature* **304**, 730-733, doi:10.1038/304730a0 (1983).

11 Kolb, H. A. & Wakelam, M. J. Transmitter-like action of ATP on patched membranes of cultured myoblasts and myotubes. *Nature* **303**, 621-623, doi:10.1038/303621a0 (1983).

12 Surprenant, A., Buell, G. & North, R. A. P2X receptors bring new structure to ligand-gated ion channels. *Trends in neurosciences* **18**, 224-229, doi:10.1016/0166-2236(95)93907-f (1995).

13 North, R. A. Molecular physiology of P2X receptors. *Physiol Rev* **82**, 1013-1067, doi:10.1152/physrev.00015.2002 (2002).

14 Brake, A. J., Wagenbach, M. J. & Julius, D. New structural motif for ligand-gated ion channels defined by an ionotropic ATP receptor. *Nature* **371**, 519-523, doi:10.1038/371519a0 (1994).

15 Valera, S. *et al.* A new class of ligand-gated ion channel defined by P2x receptor for extracellular ATP. *Nature* **371**, 516-519, doi:10.1038/371516a0 (1994).

16 Kawate, T., Michel, J. C., Birdsong, W. T. & Gouaux, E. Crystal structure of the ATP-gated P2X(4) ion channel in the closed state. *Nature* **460**, 592-598, doi:10.1038/nature08198 (2009).

17 Hattori, M. & Gouaux, E. Molecular mechanism of ATP binding and ion channel activation in P2X receptors. *Nature* **485**, 207-212, doi:10.1038/nature11010 (2012).

18 Baconguis, I., Hattori, M. & Gouaux, E. Unanticipated parallels in architecture and mechanism between ATP-gated P2X receptors and acid sensing ion channels. *Curr Opin Struct Biol* **23**, 277-284, doi:10.1016/j.sbi.2013.04.005 (2013).

19 Fountain, S. J. *et al.* An intracellular P2X receptor required for osmoregulation in *Dictyostelium discoideum*. *Nature* **448**, 200-203, doi:10.1038/nature05926 (2007).
20 Fountain, S. J., Cao, L., Young, M. T. & North, R. A. Permeation properties of a P2X receptor in the green algae *Ostreococcus tauri*. *J Biol Chem* **283**, 15122-15126, doi:10.1074/jbc.M801512200 (2008).
21 Cai, X. P2X receptor homologs in basal fungi. *Purinergic Signal* **8**, 11-13, doi:10.1007/s11302-011-9261-8 (2012).
22 Moroz, L. L., Romanova, D. Y. & Kohn, A. B. Neural vs. alternative integrative systems: Molecular insights into origins of neurotransmitters *Phil. Trans. R. Soc. B.*, in press (2020).
23 Bavan, S. *et al.* The penultimate arginine of the carboxyl terminus determines slow desensitization in a P2X receptor from the cattle tick *Boophilus microplus*. *Mol Pharmacol* **79**, 776-785, doi:10.1124/mol.110.070037 (2011).
24 Bavan, S., Straub, V. A., Blaxter, M. L. & Ennion, S. J. A P2X receptor from the tardigrade species *Hypsibius dujardini* with fast kinetics and sensitivity to zinc and copper. *BMC Evol Biol* **9**, 17, doi:10.1186/1471-2148-9-17 (2009).
25 Agboh, K. C., Webb, T. E., Evans, R. J. & Ennion, S. J. Functional characterization of a P2X receptor from *Schistosoma mansoni*. *J Biol Chem* **279**, 41650-41657, doi:10.1074/jbc.M408203200 (2004).
26 Gruenhagen, J. A., Lovell, P., Moroz, L. L. & Yeung, E. S. Monitoring real-time release of ATP from the molluscan central nervous system. *J Neurosci Methods* **139**, 145-152, doi:10.1016/j.jneumeth.2004.03.008 (2004).
27 Bavan, S., Straub, V. A., Webb, T. E. & Ennion, S. J. Cloning and characterization of a P2X receptor expressed in the central nervous system of *Lymnaea stagnalis*. *PLoS One* **7**, e50487, doi:10.1371/journal.pone.0050487 (2012).
28 Moroz, L. L. *Aplysia*. *Curr Biol* **21**, R60-61, doi:10.1016/j.cub.2010.11.028 (2011).
29 Kandel, E. R. The molecular biology of memory storage: a dialogue between genes and synapses. *Science* **294**, 1030-1038, doi:10.1126/science.1067020 (2001).
30 Surprenant, A., Buell, G. & North, R. A. P2X receptors bring new structure to ligand-gated ion channels. *Trends in neurosciences* **18**, 224-229, doi:10.1016/0166-2236(95)93907-f (1995).
31 Heyland, A., Vue, Z., Voolstra, C. R., Medina, M. & Moroz, L. L. Developmental transcriptome of *Aplysia californica*. *J Exp Zool B Mol Dev Evol* **316B**, 113-134, doi:10.1002/jez.b.21383 (2011).
32 Moroz, L. L. Localization of putative nitrergic neurons in peripheral chemosensory areas and the central nervous system of *Aplysia californica*. *J Comp Neurol* **495**, 10-20, doi:10.1002/cne.20842 (2006).
33 North, R. A. & Surprenant, A. Pharmacology of cloned P2X receptors. *Annu Rev Pharmacol Toxicol* **40**, 563-580, doi:10.1146/annurev.pharmtox.40.1.563 (2000).
34 Gourine, A. V., Llaudet, E., Dale, N. & Spyer, K. M. ATP is a mediator of chemosensory transduction in the central nervous system. *Nature* **436**, 108-111, doi:10.1038/nature03690 (2005).
35 Rubakhin, S. S., Li, L., Moroz, T. P. & Sweedler, J. V. Characterization of the *Aplysia californica* cerebral ganglion F cluster. *J Neurophysiol* **81**, 1251-1260, doi:10.1152/jn.1999.81.3.1251 (1999).
36 Floyd, P. D. *et al.* Insulin prohormone processing, distribution, and relation to metabolism in *Aplysia californica*. *J Neurosci* **19**, 7732-7741 (1999).

37 Coggeshall, R. E. A cytologic analysis of the bag cell control of egg laying in Aplysia. *J Morphol* **132**, 461-485, doi:10.1002/jmor.1051320407 (1970).
38 Kupfermann, I. Stimulation of egg laying by extracts of neuroendocrine cells (bag cells) of abdominal ganglion of Aplysia. *J Neurophysiol* **33**, 877-881, doi:10.1152/jn.1970.33.6.877 (1970).
39 Kupfermann, I. Stimulation of egg laying: possible neuroendocrine function of bag cells of abdominal ganglion of Aplysia californica. *Nature* **216**, 814-815, doi:10.1038/216814a0 (1967).
40 Hatcher, N. G. & Sweedler, J. V. Aplysia bag cells function as a distributed neurosecretory network. *J Neurophysiol* **99**, 333-343, doi:10.1152/jn.00968.2007 (2008).
41 Moroz, L. L. & Kohn, A. B. Do different neurons age differently? Direct genome-wide analysis of aging in single identified cholinergic neurons. *Front Aging Neurosci* **2**, doi:10.3389/neuro.24.006.2010 (2010).
42 Moseley, T. A., Haudenschild, D. R., Rose, L. & Reddi, A. H. Interleukin-17 family and IL-17 receptors. *Cytokine Growth Factor Rev* **14**, 155-174, doi:10.1016/s1359-6101(03)00002-9 (2003).
43 Walters, E. T. *et al.* Somatotopic organization and functional properties of mechanosensory neurons expressing sensorin-A mRNA in Aplysia californica. *J Comp Neurol* **471**, 219-240, doi:10.1002/cne.20042 (2004).
44 Moroz, L. L. *et al.* Neuronal transcriptome of *Aplysia*: neuronal compartments and circuitry. *Cell* **127**, 1453-1467, doi:10.1016/j.cell.2006.09.052 (2006).
45 Puthanveettil, S. V. *et al.* A strategy to capture and characterize the synaptic transcriptome. *Proc Natl Acad Sci U S A* **110**, 7464-7469, doi:10.1073/pnas.1304422110 (2013).
46 Cummins, S. F., Degnan, B. M. & Nagle, G. T. Characterization of Aplysia Alb-1, a candidate water-borne protein pheromone released during egg laying. *Peptides* **29**, 152-161, doi:10.1016/j.peptides.2007.07.031 (2008).
47 Cummins, S. F., Nichols, A. E., Schein, C. H. & Nagle, G. T. Newly identified water-borne protein pheromones interact with attractin to stimulate mate attraction in Aplysia. *Peptides* **27**, 597-606, doi:10.1016/j.peptides.2005.08.026 (2006).
48 Cummins, S. F., Nichols, A. E., Warso, C. J. & Nagle, G. T. Aplysia seductin is a water-borne protein pheromone that acts in concert with attractin to stimulate mate attraction. *Peptides* **26**, 351-359, doi:10.1016/j.peptides.2004.10.024 (2005).
49 Matsuo, R. *et al.* Distribution and physiological effect of enterin neuropeptides in the olfactory centers of the terrestrial slug Limax. *J Comp Physiol A Neuroethol Sens Neural Behav Physiol* **206**, 401-418, doi:10.1007/s00359-020-01400-2 (2020).
50 Furukawa, Y. *et al.* The enterins: a novel family of neuropeptides isolated from the enteric nervous system and CNS of Aplysia. *J Neurosci* **21**, 8247-8261 (2001).
51 Sasaki, K., Fujisawa, Y., Morishita, F., Matsushima, O. & Furukawa, Y. The enterins inhibit the contractile activity of the anterior aorta of Aplysia kurodai. *J Exp Biol* **205**, 3525-3533 (2002).
52 Sasaki, K., Morishita, F. & Furukawa, Y. Peptidergic innervation of the vasoconstrictor muscle of the abdominal aorta in Aplysia kurodai. *J Exp Biol* **207**, 4439-4450, doi:10.1242/jeb.01273 (2004).
53 Moroz, L. L., Sudlow, L. C., Jing, J. & Gillette, R. Serotonin-immunoreactivity in peripheral tissues of the opisthobranch molluscs Pleurobranchaea californica and Tritonia

diomedea. *J Comp Neurol* **382**, 176-188, doi:10.1002/(sici)1096-9861(19970602)382:2<176::aid-cne3>3.0.co;2-0 (1997).
54 Knudsen, B., Kohn, A. B., Nahir, B., McFadden, C. S. & Moroz, L. L. Complete DNA sequence of the mitochondrial genome of the sea-slug, Aplysia californica: conservation of the gene order in Euthyneura. *Mol Phylogenet Evol* **38**, 459-469 (2006).
55 Zimmer-Faust, R. K. ATP: a potent prey attractant evoking carnivory. *Limnol Oceanogr* **38**, 1271-1275 (1993).
56 Kohn, A. B., Moroz, T. P., Barnes, J. P., Netherton, M. & Moroz, L. L. Single-cell semiconductor sequencing. *Methods Mol Biol* **1048**, 247-284, doi:10.1007/978-1-62703-556-9_18 (2013).
57 Moroz, L. L. & Kohn, A. B. Single-neuron transcriptome and methylome sequencing for epigenomic analysis of aging. *Methods Mol Biol* **1048**, 323-352, doi:10.1007/978-1-62703-556-9_21 (2013).
58 Jezzini, S. H., Bodnarova, M. & Moroz, L. L. Two-color in situ hybridization in the CNS of *Aplysia californica*. *J Neurosci Methods* **149**, 15-25, doi:10.1016/j.jneumeth.2005.05.007 (2005).
59 Moroz, L. L. & Kohn, A. B. in *In Situ Hybridization Methods, Neuromethods* Vol. 99 (ed Giselbert Hauptmann) 293-317 (Springer Science+Business Media, 2015).
60 Trapnell, C. *et al.* Transcript assembly and quantification by RNA-Seq reveals unannotated transcripts and isoform switching during cell differentiation. *Nat Biotechnol* **28**, 511-515, doi:10.1038/nbt.1621 (2010).
61 Kim, D. *et al.* TopHat2: accurate alignment of transcriptomes in the presence of insertions, deletions and gene fusions. *Genome Biol* **14**, R36, doi:10.1186/gb-2013-14-4-r36 (2013).
62 Moroz, L. L., Gyori, J. & Salanki, J. NMDA-like receptors in the CNS of molluscs. *Neuroreport* **4**, 201-204, doi:10.1097/00001756-199302000-00022 (1993).
63 Berman, H., Henrick, K. & Nakamura, H. Announcing the worldwide Protein Data Bank. *Nat Struct Biol* **10**, 980, doi:10.1038/nsb1203-980 (2003).
64 *Schrodinger, L. The PyMOL Molecular Graphics System, Version 1.3r1*, <https://www.scirp.org/(S(vtj3fa45qm1ean45vvffcz55))/reference/ReferencesPapers.aspx?ReferenceID=1571978> (2010).
65 DeLano, W. L. *The PyMOL molecular graphics system*, <http://www. pymol. org. > (2002).
66 Kelley, L. A., Mezulis, S., Yates, C. M., Wass, M. N. & Sternberg, M. J. The Phyre2 web portal for protein modeling, prediction and analysis. *Nat Protoc* **10**, 845-858, doi:10.1038/nprot.2015.053 (2015).
67 Wagner, G. P., Kin, K. & Lynch, V. J. Measurement of mRNA abundance using RNA-seq data: RPKM measure is inconsistent among samples. *Theory Biosci* **131**, 281-285, doi:10.1007/s12064-012-0162-3 (2012).
68 Zhao, S., Ye, Z. & Stanton, R. Misuse of RPKM or TPM normalization when comparing across samples and sequencing protocols. *RNA* **26**, 903-909, doi:10.1261/rna.074922.120 (2020).
69 Abrams, Z. B., Johnson, T. S., Huang, K., Payne, P. R. O. & Coombes, K. A protocol to evaluate RNA sequencing normalization methods. *BMC Bioinformatics* **20**, 679, doi:10.1186/s12859-019-3247-x (2019).
70 North, R. A. P2X receptors. *Philos Trans R Soc Lond B Biol Sci* **371**, doi:10.1098/rstb.2015.0427 (2016).

Figures

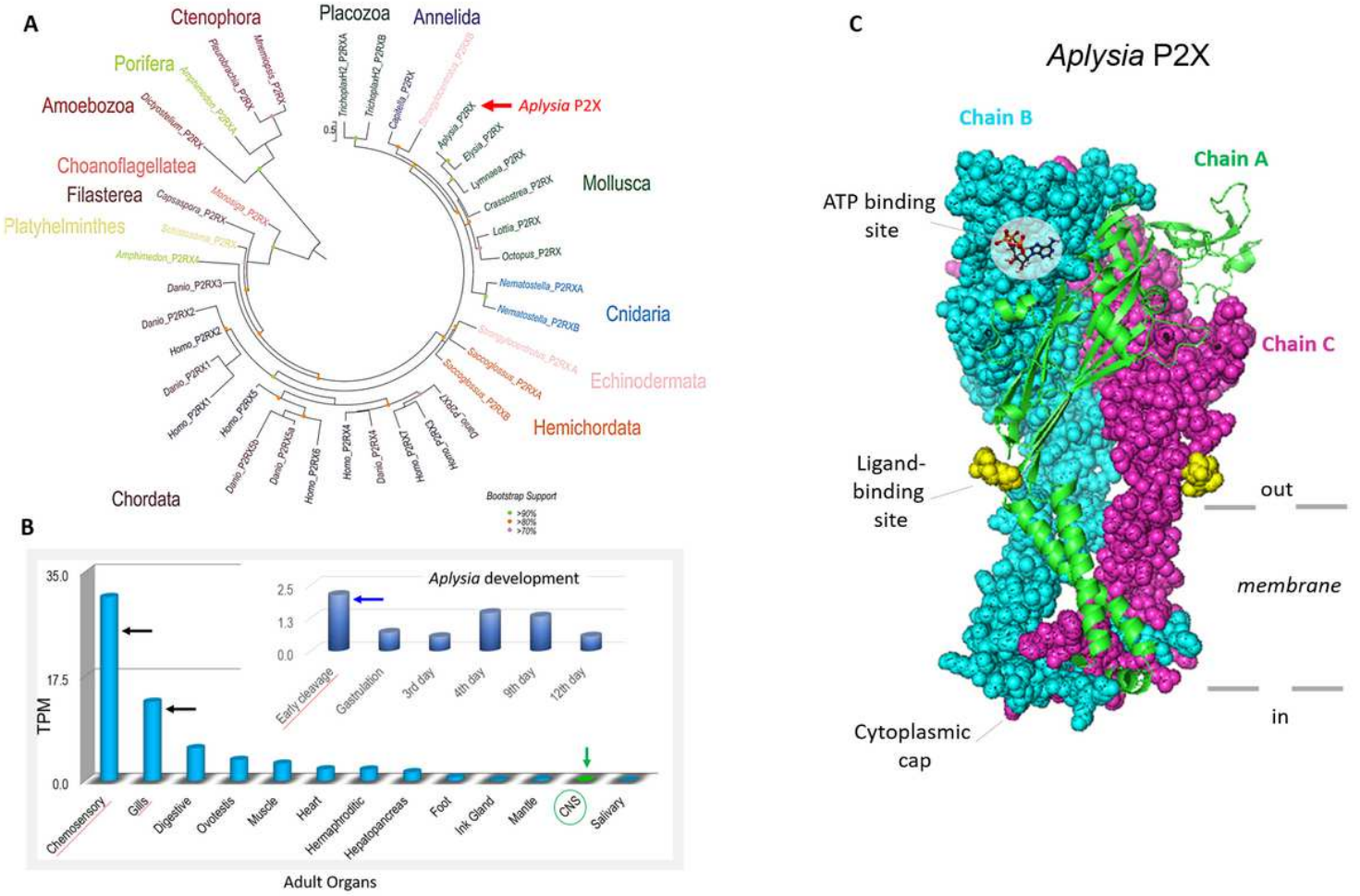

Figure 1

A. Phylogenetic relationships of P2X and P2X-like receptors (P2RX). A. A maximum likelihood (ML) phylogenetic tree of P2X receptors (Supplementary Information for sequences and accession numbers) with the best-fit model (LG+G). Bootstrap support less than 70 omitted. Phylogenetically, the P2X predicted proteins cluster by phyla. P2X-type receptors are not unique to metazoans because they are detected in unicellular green algae Ostreococcus tauri 20, the amoeba Dictyostelium discoideum 19 the unicellular eukaryote Monosiga brevicollis 20, as well as Capsaspora owczarzaki (21), and all these species, appear to have one P2X gene. Most of the non-bilaterians seem to have at least two P2X receptors (except for ctenophores, where only one receptor was detected). Lophotrochozoans, including the mollusc Aplysia and kins, appear to have one P2X receptor with different isoforms. The sea urchin and the acorn worm, Saccoglossus, both have at least two genes but numerous isoforms 1. Humans 13, as well as other chordates, appear to have seven unique P2X receptor genes 1. B. Quantification of the expression of P2X receptors in the CNS, peripheral tissues, and developmental stages (insert) of Aplysia. The RNA-seq data represented as TPM (transcript per million) values 67-69. The highest expression levels were detected in chemosensory areas (mouth areas and rhinophores), gills, and early developmental

stages (Supplementary Information, Table 1S for RNA-seq projects). C. 3D modeling for P2X receptor of A. californica (model PDB: 5svk).

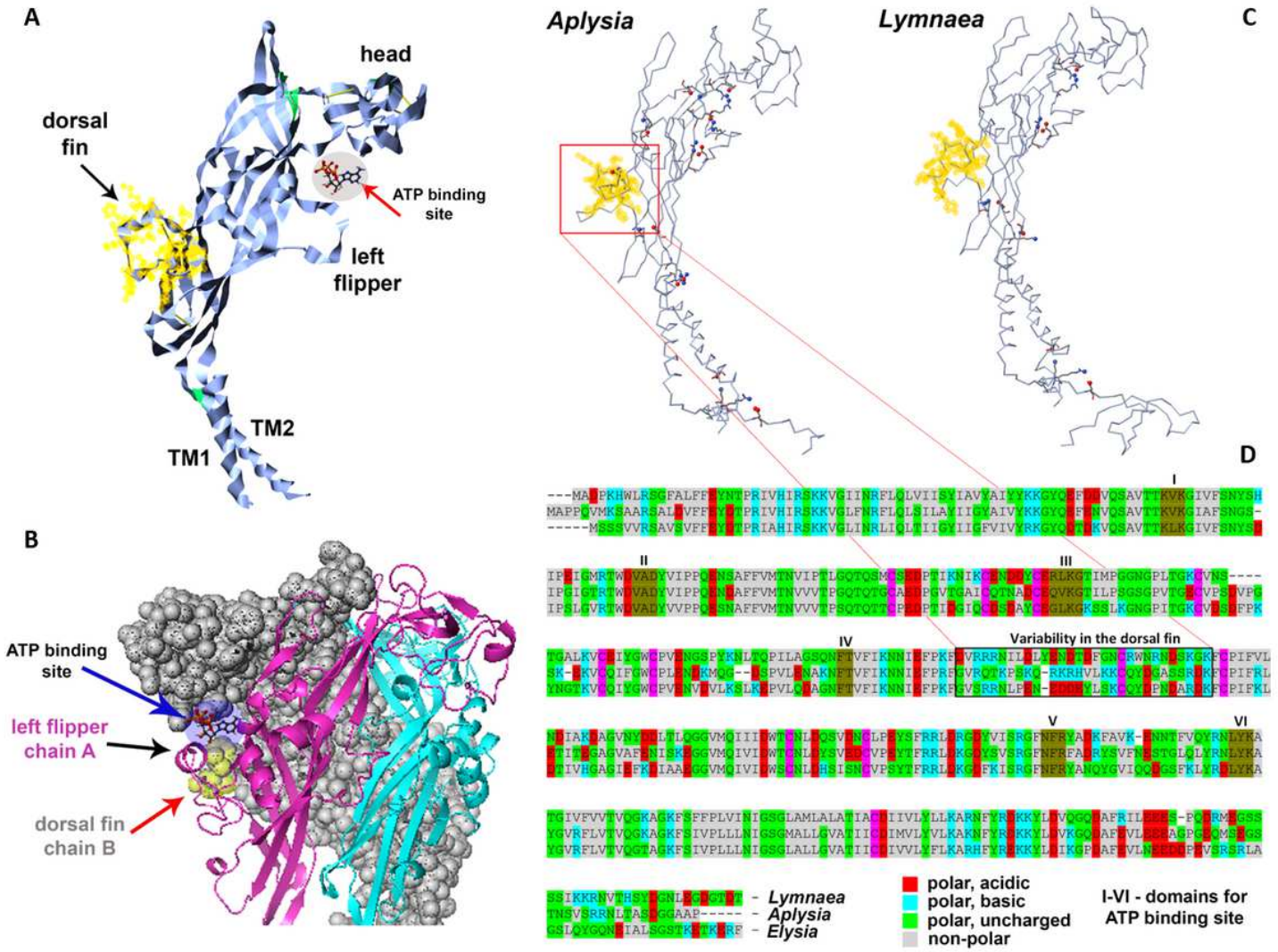

Figure 2

The organization of the P2X receptor in Aplysia californica. A and B. Structural features of the P2X monomer models with regions recognized for mammalian homologs in crystallography studies 16,17. TM1 and TM2 are transmembrane regions (see Fig. 1C). B. 3D modeling of the trimeric P2X organization with suggested functional regions16-18,70. 'Left flipper' (chain A) and 'dorsal fin' (chain B) together with a head (chain A) of these chains form the ATP binding site (see also Fig. 1C). C. Comparisons between Aplysia and Lymnaea receptors (open state) based on the difference of salt bridges (yellow – 'dorsal fin'). D. The alignment for P2X receptors in gastropod molluscs (Aplysia californica, Lymnaea stagnalis and Elysia chlorotica) with domain for the ATP binding site (brown – I-VI domains). Of note, Aplysia (middle in the alignment) has significantly less polar acidic and more polar basic amino acids in the 'dorsal fin' region [11pb:2pa] compared to other species (Lymnaea [7pb:6pa] and Elysia [5pb:8pa]), suggesting different kinetic and pharmacological properties of P2X receptors. In summary, there are 13 polar charged amino acids in the $d \text{ or } salf \in$.

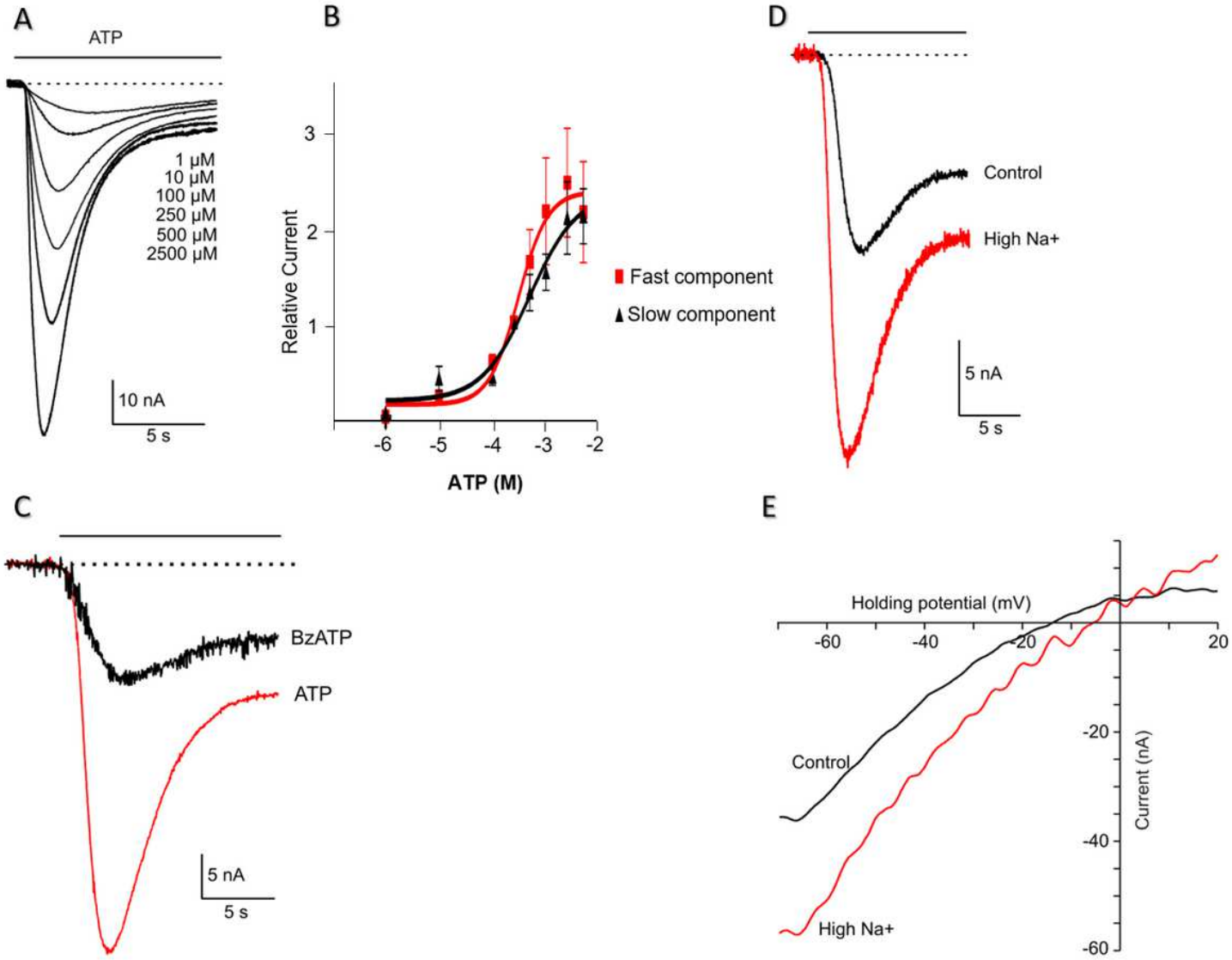

Figure 3

Functional expression of recombinant AcP2X receptors in Xenopus oocytes. A. Examples of currents recorded in response to different concentrations of ATP (HP=-70 mV, agonist application indicated by the solid line). B. Dose-response curves for ATP receptor activation. Mean currents were normalized to the response given by 250 µM ATP (n=7 oocytes). Serially increasing concentrations of ATP were applied to oocytes for 15 s at 6-min intervals. Symbols represent mean±S.E. Continuous line for ATP represents data fitted using the equation I= Imax/[1+(EC50/L)nH], where I is the actual current for a ligand concentration (L), nH is the Hill coefficient, and Imax is the maximal current (EC50fast = 306.0 µM, EC50slow= 497.4 µM; nHfast=1.58, nHslow=0.97). C. Twoelectrode voltage-clamp recordings from oocytes expressing AcP2X receptors. Representative inward currents recorded in response to ATP (red trace) and the 250 µM of Bz-ATP (HP=-70 mV, application indicated by the solid line). D. Recordings of ATP-induced current (250 µM, ATP) in the presence of normal [Na+] (96mM) and with elevated extracellular Na+ (144 mM; red trace); HP=-70 mV. E. Ramp voltage-clamp protocol from -70 mV HP to 20mV in the presence of 250µM ATP. The plots of the subtracted current (a current in the presence of ATP minus the current in the

absence of ATP) against voltage during the ramp. The red trace - high [Na+], 144 mM. According to the Nernst equation, the reversal potential was shifted by 10.2±1.3 mV to the + direction of the holding potential.

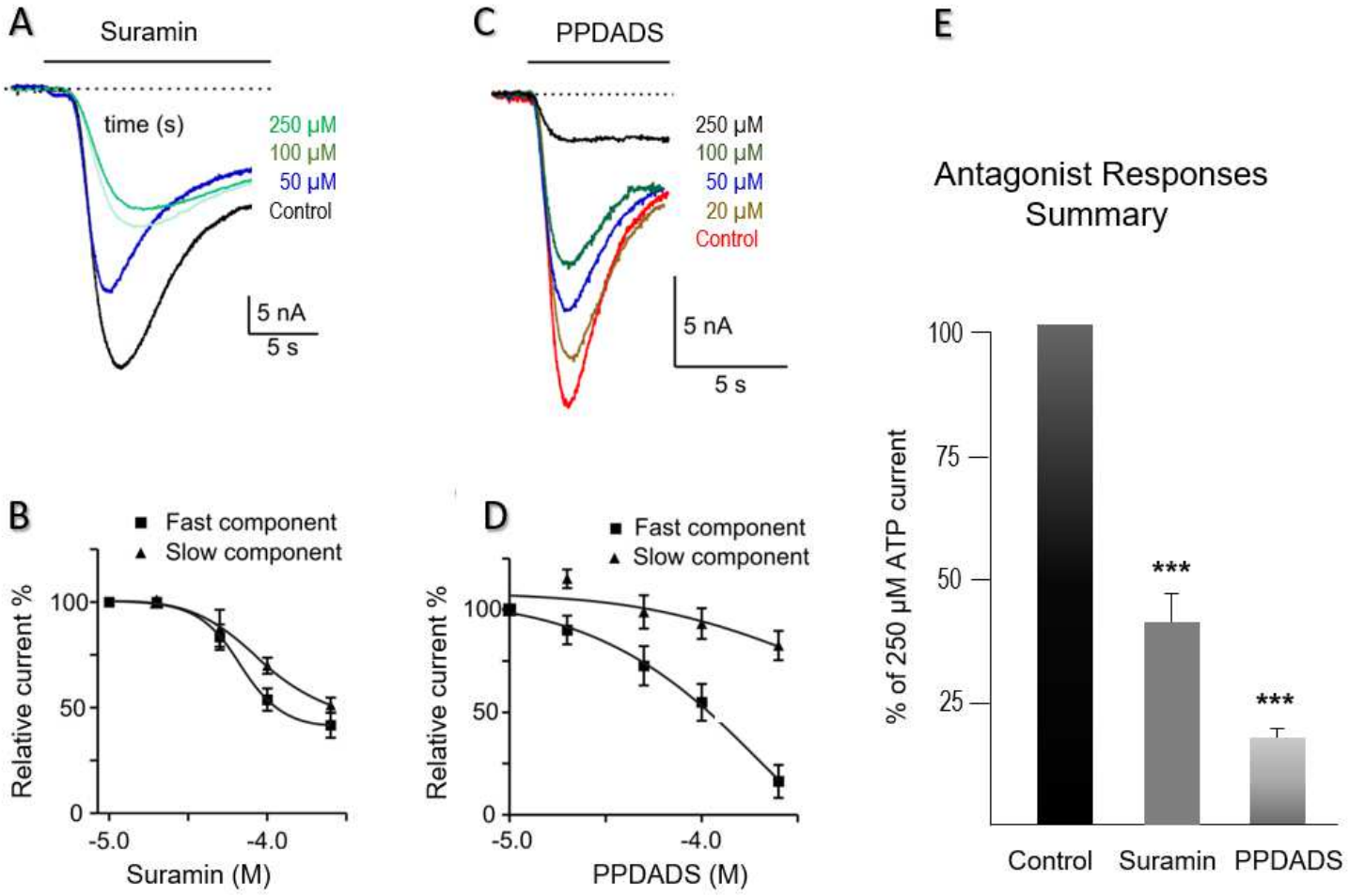

Figure 4

Pharmacology of AcP2X receptors in Xenopus oocytes. A. Example of currents induced by 250 µM ATP. ATP was applied to oocytes for 15 s, in the presence of varying concentrations of suramin (HP=-70 mV). B. Mean responses to 250 µM ATP in the presence of 1250 µM suramin. There was a suramin-resistant component of the AcP2X current. Symbols represent mean±S.E. C. Traces recorded in response to 250µM ATP in the presence of varying concentrations of the second antagonist, PPADS (concentrations are shown in µM, and all applications are indicated by the solid lines). D. Mean responses to 250µM of ATP in the presence of the PPADS (a fast component of responses - closed squares, slow component - triangles). PPADS was an effective antagonist in the range of 1–250µM. Fitting of the data using the sigmoidal dose-response curve by a continuous line, EC50fast=211.2. Symbols represent the mean±S.E. E. The suramin proved to be a more effective blocker of the ATP-activated channels among the two antagonists tested. A chart of mean currents (% of 250 µM ATP response) in the presence of 250 µM Suramin and 250 µM PPADS. Mean currents were normalized to the response given by 250 µM of ATP. Symbols represent mean±S.E; statistically significant differences (Student's t-test) from control ($P<0.05$) are indicated by asterisks (***) above the bars.

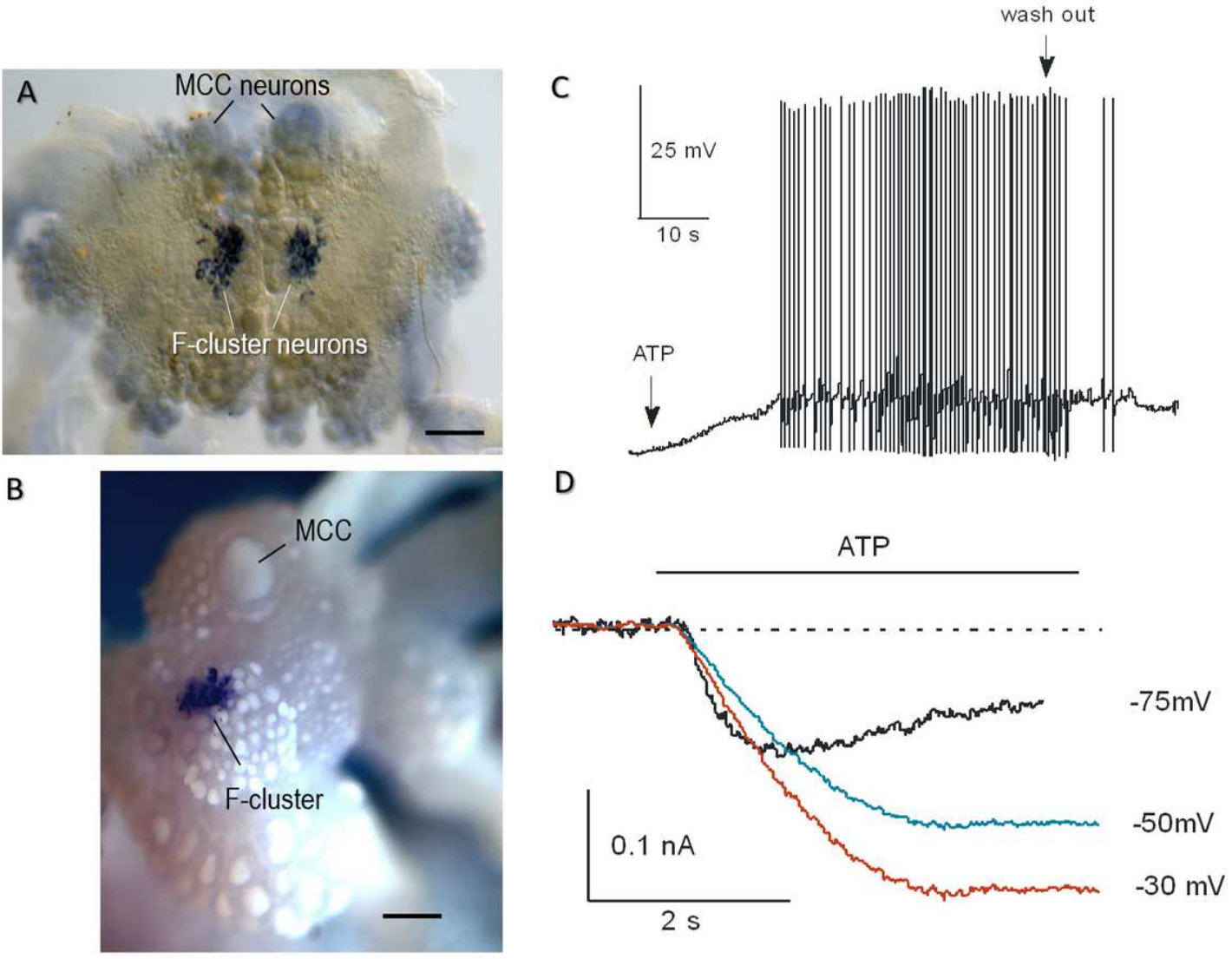

Figure 5

Distribution of AcP2X in the CNS of Aplysia and the effect of ATP on Aplysia Fcluster neurons. A and B: AcP2X is expressed in neurons of the cerebral F-cluster (in situ hybridization). A pair of giant serotonergic feeding interneurons (MCC) are indicated by arrows. A. The preparation embedded in a mounting media. B. The cerebral ganglion was photographed in 100% ethanol. Scale: 300 μm. C. Current-clamp recording from F-cluster neurons in the intact CNS. Bath application of ATP (2.0 mM) caused an excitatory response with spiking activity (2-5 mV depolarization with a burst of the action potentials), and full recovery following washout (indicated by arrows). D. Voltage-clamp recording from F-cluster neuron. Raw traces recorded in response to 2.0 mM of ATP at three holding potentials (agonist application indicated by the line).

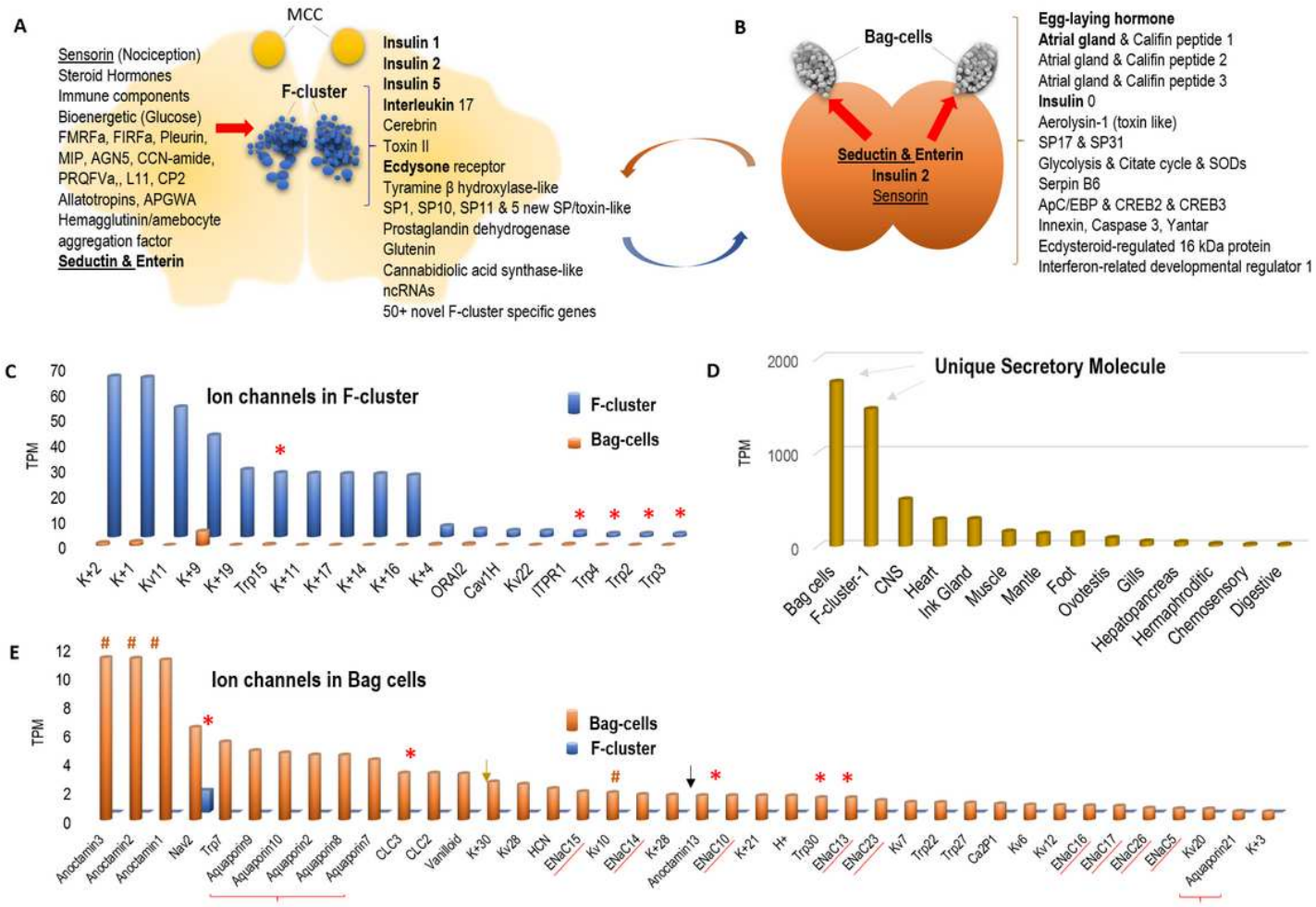

Figure 6

F-cluster and Bag cells are the two most prominent neurohaemal centers in Aplysia. A. Schematic representation of F-cluster in the cerebral ganglion (MCC- serotonergic metacerebral cells involved in feeding arousal) together with genes [on the right, e.g., insulins 1 and 2, interleukin 17, etc.] differentially expressed in this cluster (RNA-seq). Red arrow indicates predicted other peptidergic inputs [on the left] to F-cluster (see text for details). F-cluster is one of the most molecularly heterogenous neurorosecretory clusters in the CNS. B. Bag cells in the abdominal ganglion with cluster-specific peptides [on the right] expressed in these neurosecretory cells (RNA-seq). Red arrow indicates other peptidergic inputs to bag cells (see text for details). Of note, seductin, enterin, and sensorin inputs are shared (underlined) between these two neurohaemal centers, whereas insulin 2 is produced in the F-cluster. C. Both bag cells and F-cluster have the highest overall expression of an uncharacterized secretory molecule (XP_005092953.2) compared to other organs. D and E. Putative ion channels differentially expressed in the F-cluster and bag cells, respectively (see Supplementary Information excel table:Ion channels for F-cluster and Bag cells). Asterisks indicate cluster-specific transient receptor potential (TRP) channels; # - anoctamins,– aquaporins; brown and black arrows HCN and voltage-gated proton channels, respectively. ENaC – are

ligand-gated peptide channels (underlined). Other abbreviations: K+ Calcium-activated, Inwardly rectifying, Tandem pore domain potassium channels; Kv voltagegated potassium chnnels; Nav- voltage-gated sodium channel, Ca2P two pore calcium channels. The numbers in names Do Not infer type of channel but for identification only.

Supplementary Files

This is a list of supplementary files associated with this preprint. Click to download.

- graphicalabstract.png
- SupplementaryInformationP2X.pdf
- Table2SSupplementaryInformationFBagclustersRNAseq.xlsx